

*Supplemental figures for: A Gaussian process model of
human electrocorticographic data*

Lucy L. W. Owen¹, Tudor A. Muntianu¹, Andrew C. Heusser^{1,2},
Patrick Daly³, Katherine Scangos³, and Jeremy R. Manning^{1*}

¹Department of Psychological and Brain Sciences, Dartmouth College,
Hanover, NH 03755, USA

²Akili Interactive,
Boston, MA 02110, USA

January 21, 2020

References

- Combrisson E, Vallat R, O'Reilly C, Jas M, Pascarella A, l'Saive A, Thiery T, Meunier D, Altukhov D, Lajnef T, Ruby P, Guillot A, Jerbi K 2019. Visbrain: a multi-purpose GPU-accelerated open-source suite for multimodal brain data visualization. *Frontiers in Neuroinformatics* 13:1–14.
- Rubin T N, Kyoejo O, Gorgolewski K J, Jones M N, Poldrack R A, Yarkoni T 2017. Decoding brain activity using a large-scale probabilistic functional-anatomical atlas of human cognition. *PLoS Computational Biology* 13:e1005649.
- Yeo B T T, Krienen F M, Sepulcre J, Sabuncu M R, Lashkari D, Hollinshead M, Roffman J L, Smoller J W, Zollei L, Polimieni J R, Fischl B, Liu H, Buckner R L 2011. The organization of the

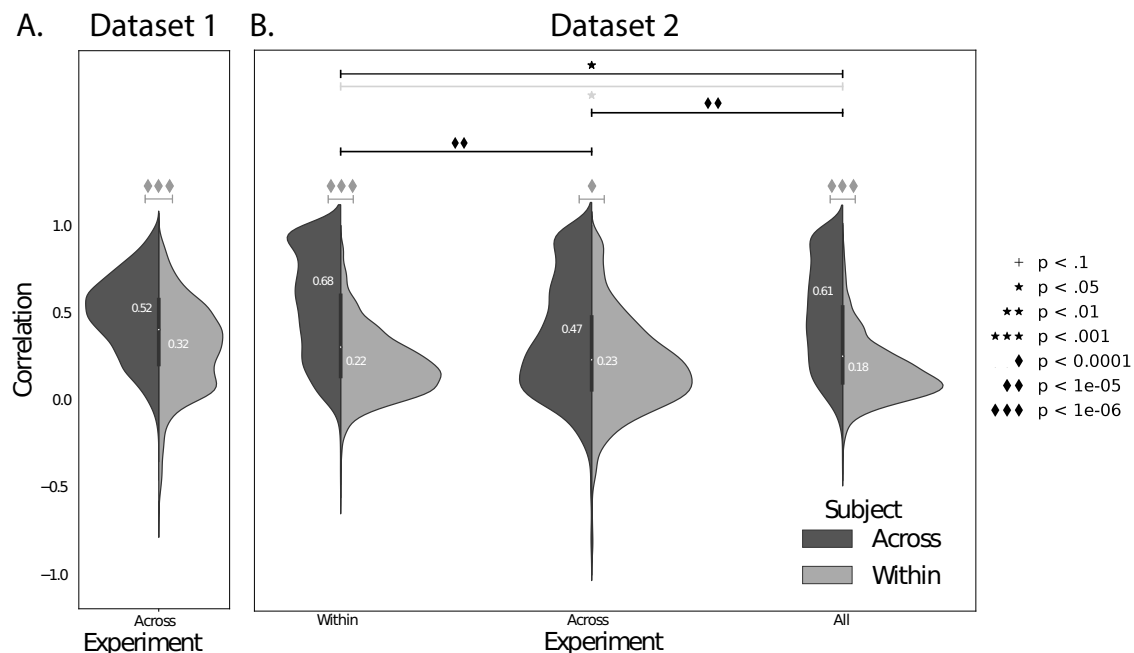


Figure S1: Reconstruction quality for Datasets 1 and 2. **A.** Distributions of correlations between observed versus reconstructed activity by electrode, for Dataset 1. The split violin plot reflects the same data as Figure 3A, presented here for comparison. **B.** Distributions of correlation between observed versus reconstructed activity by electrode, for Dataset 2. The left-most split violin plot (“Within”) reflects the same data as Figure 3B, presented here for comparison. The “Across” plot reflects the same analyses, but limited to models that were trained and tested on *different* Dataset 2 experiments. The “All” plot reflects the same analyses, but including models that were trained and tested on both of the Dataset 2 experiments. All plots: the dark gray distributions denote across-subject correlations (model trained on all but one patient and tested on the held-out patient), and the medium gray distributions denote within-subject correlations (model trained on all but one electrode from one patient, and tested on the held-out electrode). The horizontal bars denote *t*-tests between the corresponding distributions (after *z*-transforming the correlations), and the white numbers reflect the distribution means. The symbols denote the corresponding *p*-values of those statistical tests.

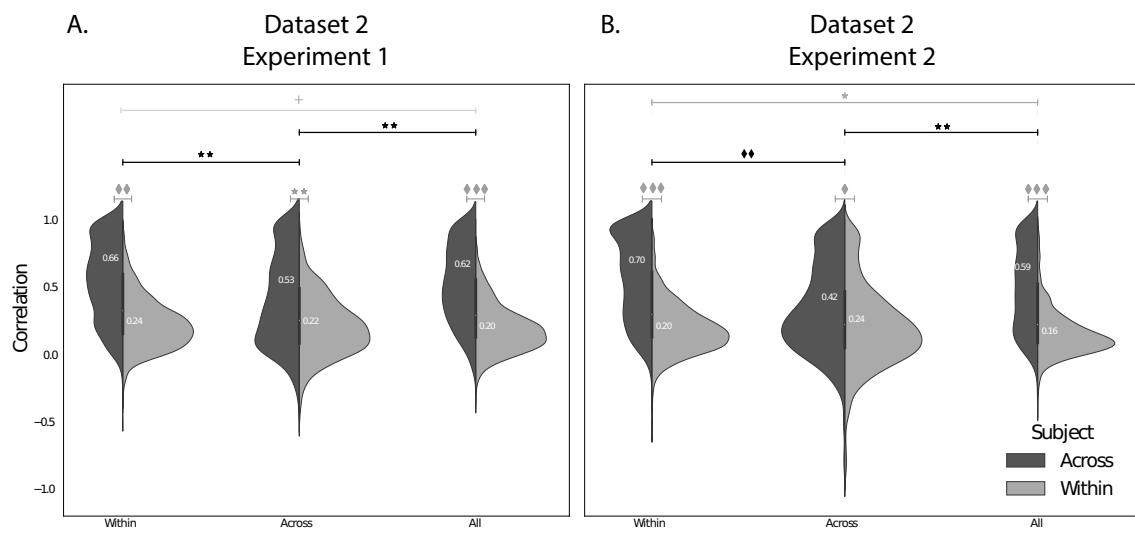


Figure S2: Reconstruction quality for Dataset 2, Experiments 1 and 2. **A. Distributions of correlations between observed versus reconstructed activity by electrode, for Experiment 1.** Each split violin plot and horizontal bar is in the same format as the plots in Figure S1. “Within” denotes within-subject correlations (model trained on all but one electrode from one patient, and tested on the held-out electrode); “Across” denotes across-subject correlations (model trained on all but one patient and tested on the held-out patient); “All” denotes a model trained on all data from all patients, except for one held-out electrode (and tested on the held-out electrode). **B. Distributions of correlations between observed versus reconstructed activity by electrode, for Experiment 2.** All of the plots and bars are in the same format as those in Panel A.

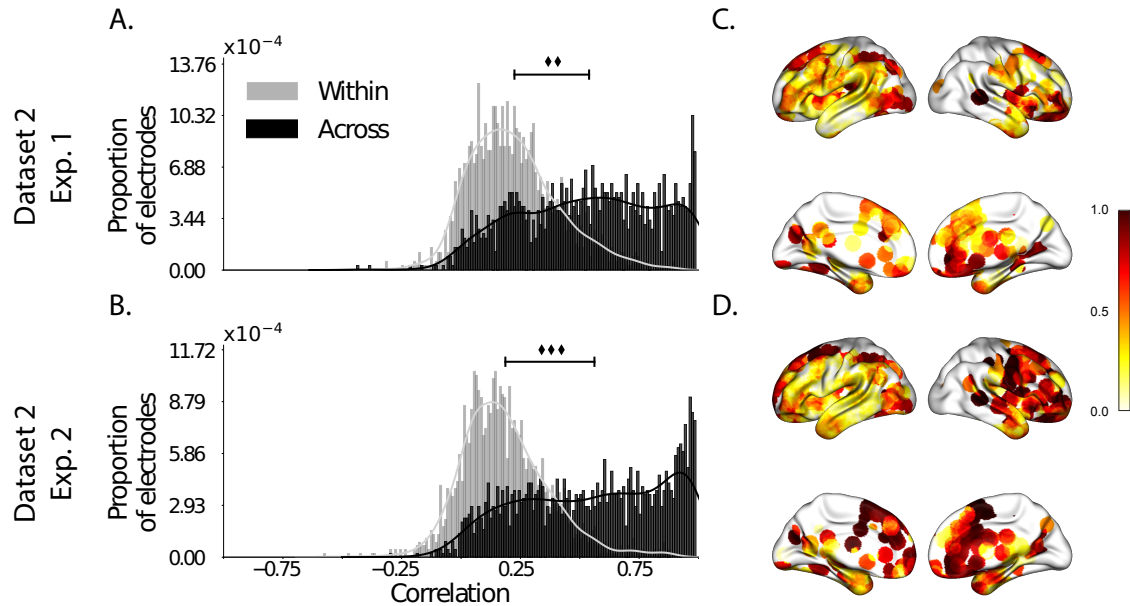


Figure S3: Reconstruction quality across all electrodes in two Dataset 2 experiments. **A. Distributions of correlations between observed versus reconstructed activity by electrode, for Experiment 1.** Same format as Figure 3A and B, but reflects data shown in Figure S2A (leftmost violin plot). **B. Distributions of correlations between observed versus reconstructed activity by electrode, for Experiment 2.** Same format as Figure 3A and B, but reflects data shown in Figure S2B (leftmost violin plot). **C.-D. Reconstruction performance by location.** Each dot reflects the location of a single implanted electrode from Dataset 2, Experiment 1 (Panel C) or Dataset 2, Experiment 2 (Panel D). The dot colors denote the average within-experiment (across-session) correlation, using the across-patient correlation model, between the observed and reconstructed activity at the given electrode location projected to the cortical surface (Combrisson et al., 2019).

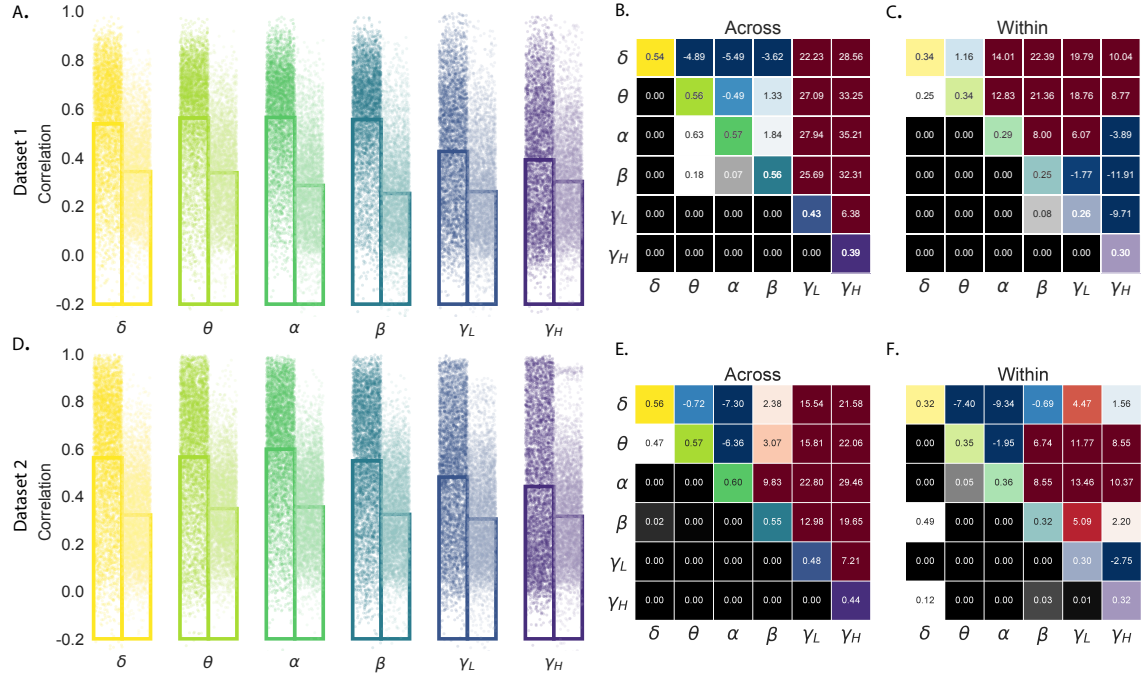


Figure S4: Reconstruction quality across all electrodes in two ECoG datasets for each frequency band.

A. Distributions of correlations between observed versus reconstructed activity by electrode, for each frequency band in Dataset 1. Same format as Figure 5A, but using power at each frequency. **B.** Statistical summary of across-patient reconstruction quality by electrode for each frequency band in Dataset 1. Same format as Figure 5B, but using power at each frequency. **C.** Statistical summary of within-patient reconstruction quality by electrode for each frequency band in Dataset 1. This panel displays the within-patient statistical summary, in the same format as Panel B. **D.** Distributions of correlations between observed versus reconstructed activity by electrode, for each frequency band in Dataset 2. This panel displays reconstruction accuracy distributions for each frequency band for Dataset 2. **E.** Statistical summary of across-patient reconstruction quality by electrode for each frequency band in Dataset 2. This is the same format as Panel B for Dataset 2. **F.** Statistical summary of within-patient reconstruction quality by electrode for each frequency band in Dataset 2. This is the same format as Panel C for Dataset 2.

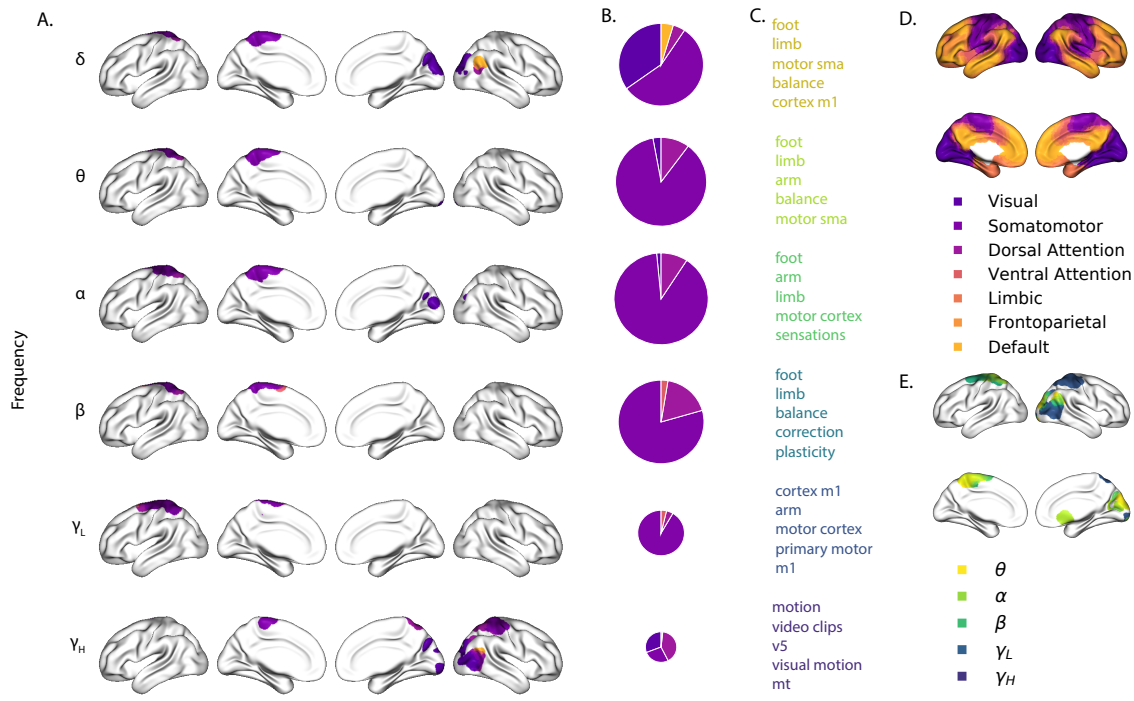


Figure S5: Most informative electrode locations by frequency and the networks involved. **A. Intersections across datasets for each frequency.** Same format as Figure 6A, but using power at each frequency. **B. Proportion of networks in most informative electrode locations by frequency.** Pie graphs display the proportion of the 7 networks (Yeo et al., 2011) in the most informative locations by frequency, and are sized relative to the average reconstruction accuracy for each frequency. **C. Terms associated with most informative electrode locations.** The lists of terms display the top five Neurosynth terms (Rubin et al., 2017) decoded from the corresponding brain maps, and colored according the frequency (see Panel E legend). **D. Network parcellation from (Yeo et al., 2011).** Seven network parcellation as described in (Yeo et al., 2011). **E. Most informative locations by frequency.** The inflated brain plot displays the locations of the most informative locations (Panel A), colored by frequency, and projected onto the cortical surface (Combrisson et al., 2019).

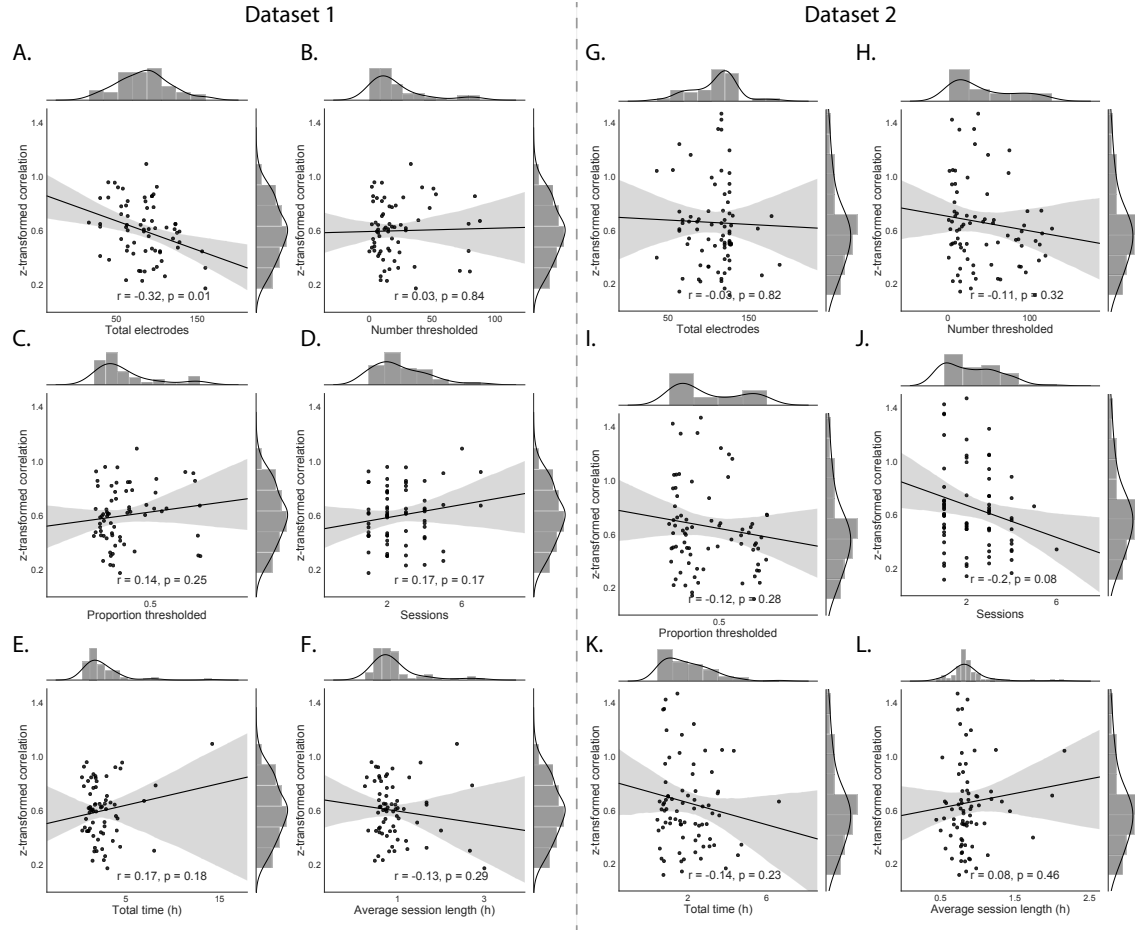


Figure S6: Reconstruction accuracy versus within-subject data features for two ECoG datasets. A.-F. Features from Dataset 1. Features include: (A.) total number of electrodes implanted in each patient's brain, (B.) per-patient number of electrodes that were filtered out due to having an maximum kurtosis greater than 10 across all recording sessions, (C.) per-patient proportion of electrodes that were filtered out due to having an average kurtosis greater than 10, (D.) per-patient number of recording sessions, (E.) per-patient total recording time (h), and (F.) per-patient average session length (h). **G.-L. Features from Dataset 2.** Analogous format to Panels A-F.

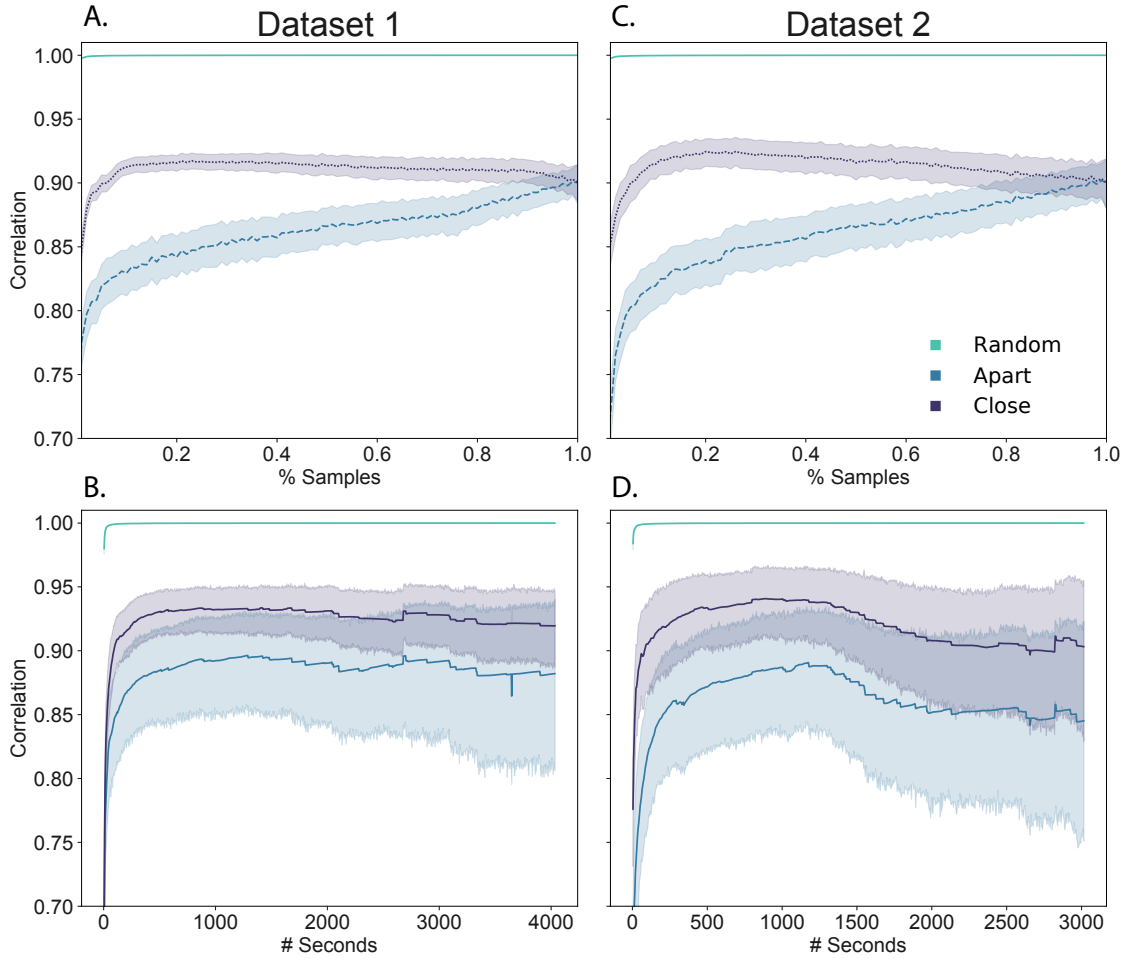


Figure S7: Stability of correlation matrix across time. **A.–B. Features from Dataset 1.** Features include: **(A. Correlation of split halves by the percent samples included.)** For each patient, we split the timeseries data in half and created a correlation matrix with one half. With the remaining data, we created the second correlation matrix with more and more time samples (in 1000 sample increments). These time samples were either drawn randomly (“Random”), or were drawn sequentially from either the closest timepoint (“Close”) or the furthest timepoint (“Apart”). The two correlation matrices were then correlated, and the coefficient plotted relative to the percentage of data included. **(B. Correlation of split halves by the number of time samples included.)** Same analysis as Panel A, but the coefficient plotted relative to the total number of samples included. **C.–D. Features from Dataset 2.** Analogous format to Panels A–B.

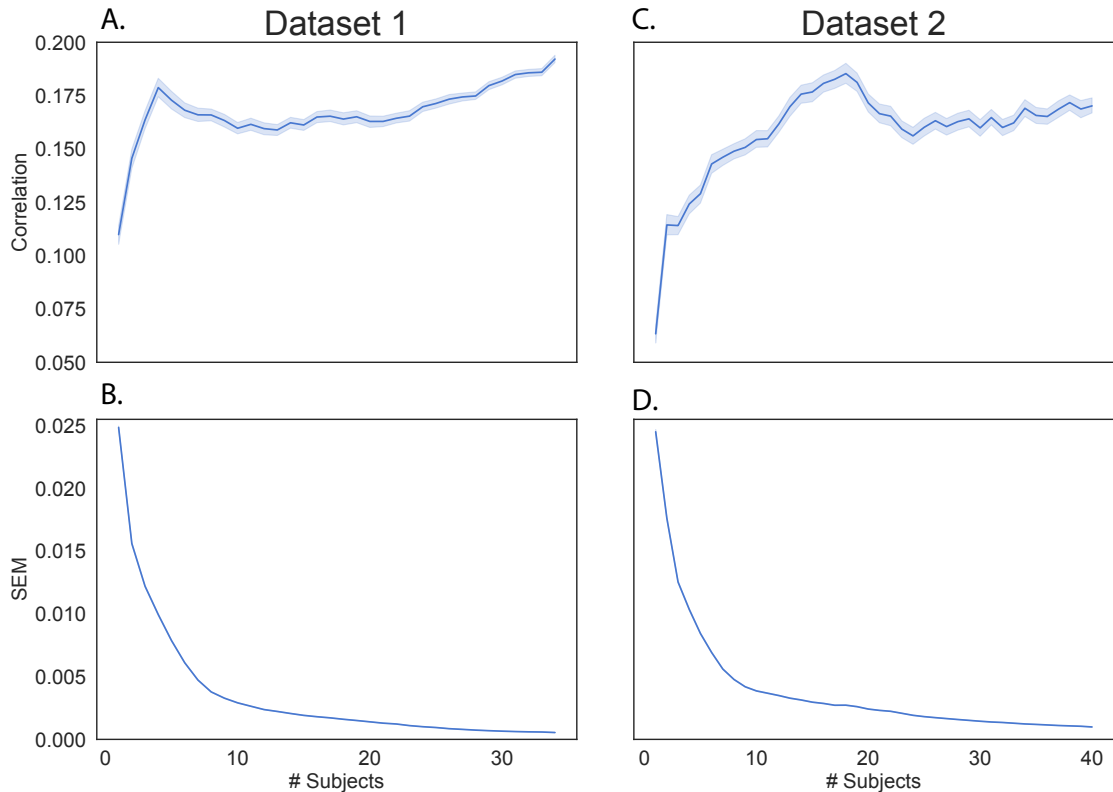


Figure S8: Stability of correlation matrix across patients. **A.–B. Features from Dataset 1.** Features include: **(A. Correlation of split halves by number of patients included.)** For 500 iterations, we randomly split the patient-specific correlations in half, then created one correlation matrix with the first half and created the second correlation matrix using more and more patients. The two correlation matrices were then correlated, and the coefficient plotted relative to the number of patients included. **(B. Standard error of the mean across iterations by the number of patients included.)** To measure the variability across the iterations, we plot the standard error of the mean as a function of the number of patients included in the second correlation matrix. **C.–D. Features from Dataset 2.** Analogous format to Panels A–B.

human cerebral cortex estimated by intrinsic functional connectivity. *Journal of Neurophysiology* 106:1125–1165.